PIER C

(Received 12 October 2025, Accepted 13 November 2025, Scheduled 6 December 2025)

A Two-Port Triple Band Beam Steering Leaky-Wave Corrugated Antenna for Millimeter Wave Applications

Nidhi Tewari*, Abhay Kumar, Nitin Muchhal, and Shweta Srivastava

Department of Electronics and Communication Engineering, Jaypee Institute of Information Technology, Noida, India

ABSTRACT: A pattern reconfigurable wideband leaky wave corrugated antenna is designed and presented in this paper. The proposed antenna shows a beam steering performance. The proposed antenna is designed using transverse periodic logarithmic slots at the top layer and longitudinal periodic leaky wave slots at the bottom ground layer. The transverse leaky wave antenna radiates in end fire direction at 25.9 GHz and 27.3 GHz. The longitudinal periodic slots on the antenna's bottom metal layer provides broadside radiation at 24.7 GHz. The leaky wave antenna scans beam at 90°, -90°, 159°, and -160° by varying the port excitation. The proposed antenna design is suitable for millimeter wave applications.

1. INTRODUCTION

The rapid growth of satellite communications, high-frequency radar systems, and 5G networks has spurred a demand for compact, efficient, and highly reconfigurable antennas operating in the Ka-band (26.5–40 GHz). Among various antenna technologies, leaky wave antennas (LWAs) have garnered significant interest due to their inherent capabilities for beam steering, high directivity, and simple planar design. These features make LWAs ideal for applications requiring dynamic beam steering and reconfigurable radiation patterns. Low-profile antennas with pattern reconfigurability are an indispensable part of modern communication systems [1], and therefore, low-profile beam-steerable antennas are increasingly gaining popularity. To improve signal-to-noise ratio (SNR) and spatial resolution, a beam-steerable antenna concentrates the radiated power in a narrow beam in a particular direction.

To improve coverage and track a wider region, it steers the angle of its beam. Beam-steerable antennas, particularly at high frequencies, have become vital components in defence, image sensing, and communication due to their ability to reduce the number of components, cost, and complexity of hardware. A promising approach to enhance the versatility and functionality of LWAs is the integration of quarter stub structures, which enable fine-tuned control over radiation characteristics. This adaptability is crucial in environments where dynamic frequency allocation and spatial filtering are essential, such as in dense satellite constellation and advanced radar systems.

Recently, leaky wave antennas (LWAs) have been widely studied and designed for reconfigurability applications. Javanbhakt et al. [6] proposed a fixed frequency beam-steering LWA. Through narrow offset longitudinal slots engraved on a substrate integrated waveguide (SIW) [4], radiation is produced. A novel SIW leaky wave antenna with end fire radiation and suppressed side lobe at centre frequency of 11.8 GHz was proposed by Liu et al. [7]. Its upper and bottom planes were etched with Taylor tapered transverse slots. A substrate integrated waveguide based LWA was proposed by [8] that provided low cross polarized continuous beam scanning from backward to forward with a frequency sweep from 7.5 to 10.75 GHz. It was achieved by shorting only upper edge of the top plane to the ground plane and engraving uniform periodic transverse slots at centre of the upper plane. In [9], the authors proposed a Leaky wave antenna with broadside radiation for CubeSat applications. In order to accomplish broadside radiation in the far-field at two different frequencies (23.3 GHz and 25.2 GHz), the compact structure made use of shorting walls and centre feeding [10]. Some beam scanning reconfigurable LWAs based on a corrugated substrate integrated waveguide (CSIW) were recently presented by [11–16]. Periodic open stubs corrugated antennas are gaining popularity among researchers, which overcome the fabrication challenge that is filling of copper in metallic vias of SIW [23, 24]. This limitation overcomes the designing of SIW antennas for millimeter wave frequency region as the design of antenna becomes more compact and miniaturized. A vias-less technology was introduced to overcome this challenge [18, 19].

A wideband, beam-steerable leaky-wave antenna based on an open-circuited periodic stub (corrugated) structure operating in the Ka-band is presented. The proposed design leverages the interplay between the leaky wave phenomenon and corrugated antenna to achieve highly reconfigurable beam patterns. The proposed antenna characterized by its ease of fabrication, low profile, and capability for integration into planar circuit technologies. Comprehensive simulations and experimental validations confirm the efficacy of the design, showcasing its potential for high-performance Ka-band applications. The proposed antenna is simulated using Ansys HFSS ver 2023 simu-

* Corresponding author: Nidhi Tewari (nidhi.tewari@mail.jiit.ac.in).

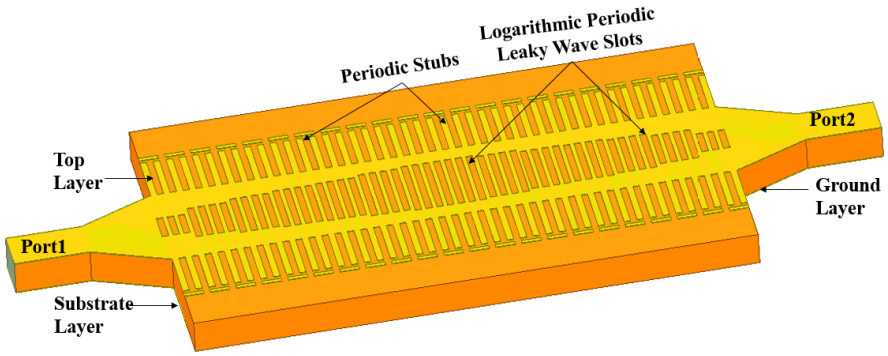

FIGURE 1. Proposed antenna design layout.

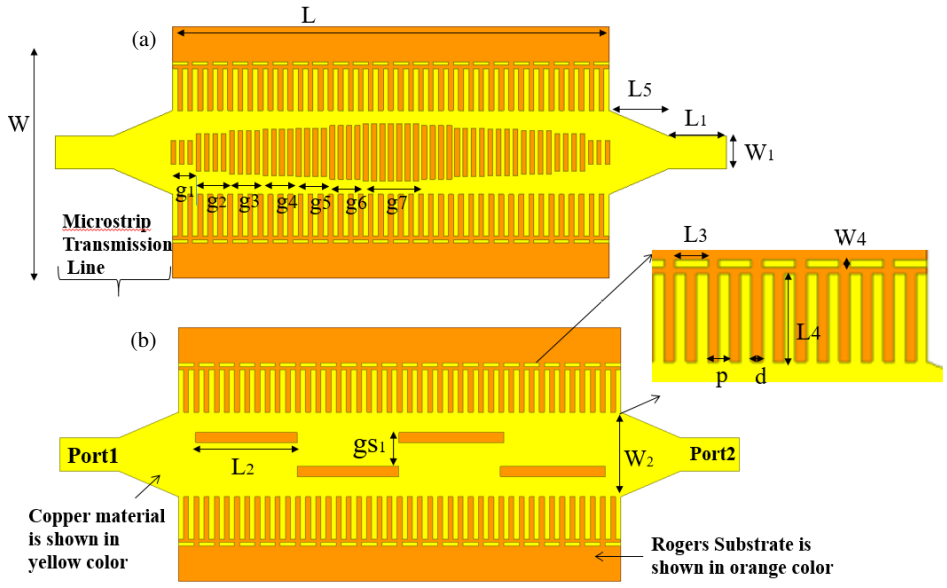

FIGURE 2. Configuration of leaky wave periodic stub antenna. (a) Top layer, (b) bottom layer. Design parameters are $L = 26.1$ mm, $W = 15$ mm, $L_1 = 3.5$ mm, $W_1 = 2$ mm, $L_2 = 6$ mm, $W_2 = 5$ mm, $L_3 = 0.9$ mm, $L_4 = 2.5$ mm ,$W_4 = 0.2$ mm, $L_5 = 3.5$ mm, $gs_1 = 2$ mm, $s_1 = 1.4$ mm, $s_2 = 2.2$ mm, $s_3 = 2.6$ mm, $s_4 = 2.8$ mm, $s_5 = 2.9$ mm, $s_6 = 3.2$ mm, $s_7 = 3.4$ mm, $g_1 = 1.3$ mm, $g_2 = 1.8$ mm, $g_3 = 1.8$ mm, $g_4 = 1.8$ mm, $g_5 = 1.8$ mm, $g_6 = 1.8$ mm, $g_7 = 3.3$ mm, $p = 0.6$ mm, $d = 0.3$ mm. (Here s_1, s_2, s_3, s_4, s_5, s_6 and s_7 are length of the leaky wave periodic slots gradually increasing).

lation software, fabricated using PhCNC machine, tested using Vector Network Analyzer and anechoic chamber. The paper is categorized into following sections. Section 1 covers introduction. Section 2 covers design methodology and its design parameters. Section 3 covers the analysis of design evolution, comparison of designs, measured and simulated result analysis, and Section 4 is the conclusion.

2. ANTENNA DESIGN METHODOLOGY

2.1. Corrugated Periodic Stub Antenna Design

The proposed antenna design, shown in Fig. 1, consists of three layers: top, substrate, and bottom layers. The bottom layer is conducting copper (thickness of 35 µm) with periodic stubs; second layer is substrate Rogers RT Duroid 5880 (thickness of 1.57 mm) of 2.2 dielectric constant and loss tangent of 0.0009; and top layer is a replica of bottom layer with approximately $\lambda/4$ length periodic stubs.

The antenna is fed by a microstrip tapered transition of 50 ohm characteristic impedance. The leaky wave periodic stub antenna design is shown in Fig. 2. The two port feeding is done using a microstrip tapered transition of length $\lambda/4$ ('L_5') equal to 3.5 mm. The width of the microstrip line is denoted as 'W_1' and length as 'L_1', respectively. The microstrip tapered transmission line is designed by using equations given in [17]. Instead of using traditional metallic via holes like in SIWs (Substrate Integrated Waveguide) (dominant mode TE_{10}), open-circuited periodic stubs are employed in the proposed design to form an artificial electric wall, and stubs are characterized by length 'L_4', width of 0.3 mm each, and spacing of 'p'. The dimensions 'p' and 'd' are generally much smaller than λ_g and calculated using principles similar to those of traditional SIWs [5]. The smaller stubs of length 'L_3' of 0.9 mm are placed at the end edges of open circuited stubs to mini-

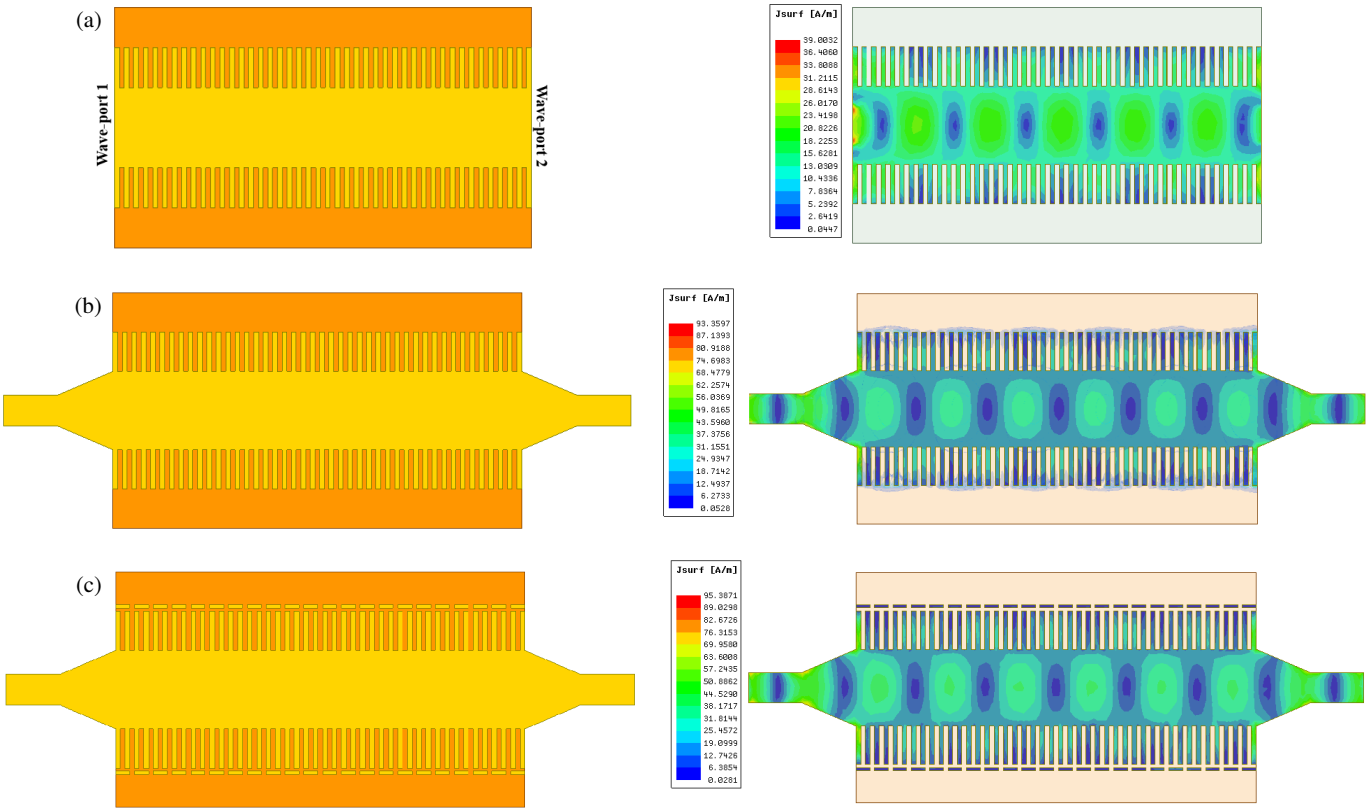

FIGURE 3. Design steps followed to design a leaky wave periodic stub corrugated antenna with minimum surface current leakage and better transmission of guided waves, (a) Design A, (b) Design B and (c) Design C.

mize the electric field leakage. The top and bottom planes both are designed with symmetrical open circuited stubs, allowing the propagation of guided waves along the artificial walls from port 1 to port 2 and vice versa. The dominant mode of proposed design is TE_{10}. The width 'W_1' is calculated using an equation given in [5]. The overall dimension of proposed antenna is 15 mm × 26.1 mm × 1.57 mm.

2.2. Leaky Wave Transverse/Longitudinal Slots Design

Leaky wave antennas (LWAs) [2, 20–22] are travelling wave antennas. On a guiding framework, a traveling wave travels but leaks through a radiating aperture. Leaky wave radiation often emanates from a closed waveguide that has some sort of periodic or continuous power outflow into the surrounding area. For radiation to exist, a fast mode of propagation is required with $\beta < ko$, where β is the modal phase constant. The speed of light is less than phase velocity in a fast wave region. The main radiation beam is directed along $\theta = \sin^{-1}\frac{\beta}{ko}$ where θ is measured from broadside. Leaky-wave antennas (LWAs) have distinguished frequency-scanning characteristics, which make them beam-steerable by nature. When power leaks through slot into free space from the traveling wave in the guiding structure, they radiate, and when the frequency alters, beam is scanned [3]. Leaky wave slots enable a guided traveling wave to flow along the walls of the antenna structure. The top layer of the antenna is a copper metal which consists of logarithmic rectangular leaky slots with group of g_1 *(three slots)*, g_2 *(four slots)*, g_3 *(four slots)*, g_4 *(four slots)*, g_5 *(four slots)*, g_6 *(four slots)*, g_7 *(seven slots)* in increasing length and then decreases to $g_6, g_5, g_4, g_3, g_2, g_1$. The width of each slot remains constant 0.3 mm. The top plane leaky wave slots are transverse, where the bottom consists of longitudinal slots of length 'L_2', and the separation between slots is 'gs_1', as shown in Fig. 2. The four longitudinal slots are placed at equidistance to both the ports for proper impedance matching of antenna.

3. RESULT ANALYSIS & DISCUSSION

3.1. Evolution of Leaky Wave Periodic Stub Corrugated Antenna

Figure 3(a) shows "design A" consisting of periodic open circuited stubs of length approximately $\lambda/4$. On the excitation of antenna at port 1, wave is guided along the length of the guiding artificial walls towards port 2. The "design A" antenna resonates at 26.54 GHz with the return loss of 19.7 dB and insertion loss of 2 dB. Here, S_{21} is high as −5.74 dB at 25.02 GHz, which means that there is insufficient transfer of power from port 1 to port 2 or leakage of radiation due to fringing field effects from open ends of quarter stubs, which can be seen and verified from field distribution plot shown in Fig. 3(a) and Fig. 4 S-parameter plot. In order to improve the transmission of power and the impedance matching of antenna, a microtsrip tapered transmission It improves the matching of antenna and transmission of wave from port 1 to port 2. "Design B" achieves two resonant frequency bands at 24.54 GHz and

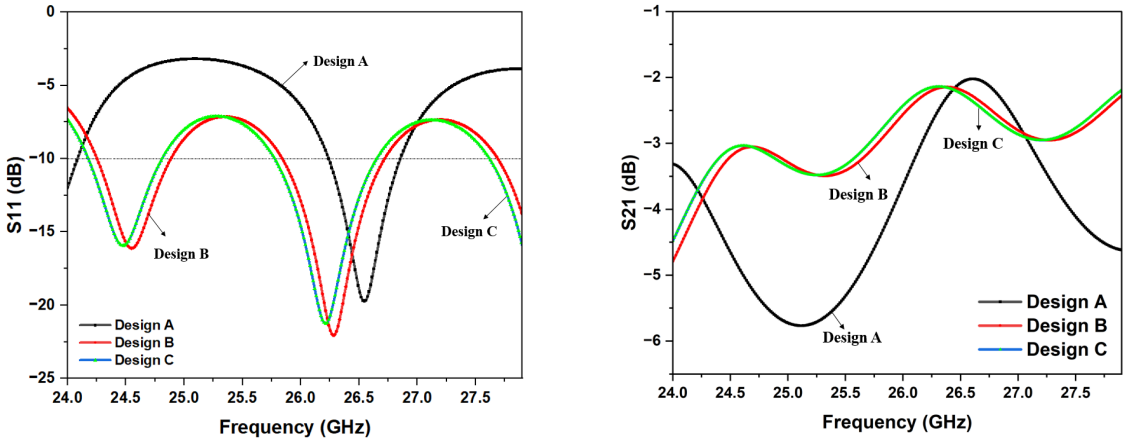

FIGURE 4. Comparison between S_{11} and S_{21} parameters of Design A, Design B, and Design C.

TABLE 1. Comparison of antenna parameters with direction of radiation for each antenna step designed when port 1 is excited.

Antenna Design	Resonant Frequency (GHz)	Return Loss (dB)	Peak Gain (dBi)	Direction of Radiation Pattern
Design C (without any slot)	24.4	15.9	6.6	End Fire
	26.2	21.2	5.4	End Fire (High SLL)
	28.0	21.2	3.7	End Fire (High SLL)
Leaky wave corrugated design with transverse top slots	24.6	17.27	4.4	End Fire
	25.9	20.9	6.6	End Fire
	27.2	22.5	6.2	End Fire
Leaky wave corrugated design with top (transverse) and bottom (longitudinal) slots	24.7	14.38	8	Broadside
	25.9	18.77	7.1	End Fire
	27.3	21.39	7	End Fire

26.29 GHz with the return losses of 16.5 dB and 22.5 dB, insertion losses of 3.1 dB and 2.13 dB, seen in Fig. 4.

To further reduce insertion loss, rectangular stubs of length 'L_3' = $0.072\lambda_o$ are implemented, where 'λ_o' is the operating wavelength at 24 GHz. The stubs are placed at edges of open circuited periodic stubs at the gap of 0.2 mm to minimize leakage and radiation losses (see Design C in Fig. 3(c)). Slight improvement in insertion loss can be seen in Fig. 4 (S_{21} plot), with a shift of resonant frequency towards lower side. An antenna operates at resonant frequency bands of 24.48 GHz and 26.22 GHz with return losses of 15.93 dB and 21.23 dB, and insertion losses of 3.07 dB and 2.14 dB.

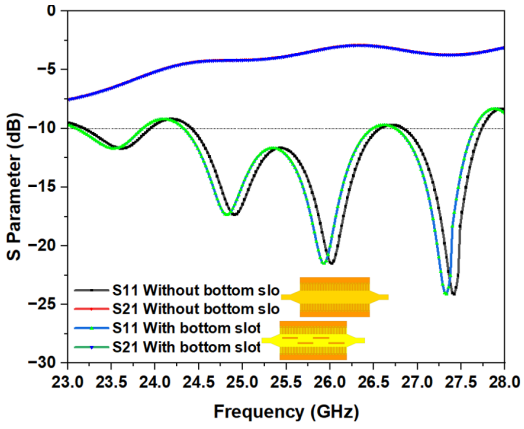

FIGURE 5. Comparison between S_{11} and S_{21} without and with periodic longitudinal slots at the bottom plane of antenna (S_{21} for both cases are overlapping).

3.2. Analysis of Proposed Leaky Wave Periodic Stub Corrugated Antenna Design

In Fig. 5, a comparison of corrugated antennas without and with bottom slots is shown. In both the cases, the antenna resonates at three bands with approximately same impedance matching. A slight shift of frequency and low return loss are observed because the length of slots at the bottom is $\lambda/2$ where λ is the operating wavelength at 24.7 GHz. From Table 1, it is clear that antenna radiates in approximately broadside and end fire directions. The periodic logarithmic longitudinal leaky-wave slots on the top layer, along with the transverse periodic slots on the bottom layer, enable antenna radiation at 23.5 GHz, 24.7 GHz, 25.9 GHz, and 27.32 GHz. The number and placement of slots on the top plane are optimized to achieve beam steering, since the slot position and dimensions influence the phase variation of the wave by altering its effective wavelength.

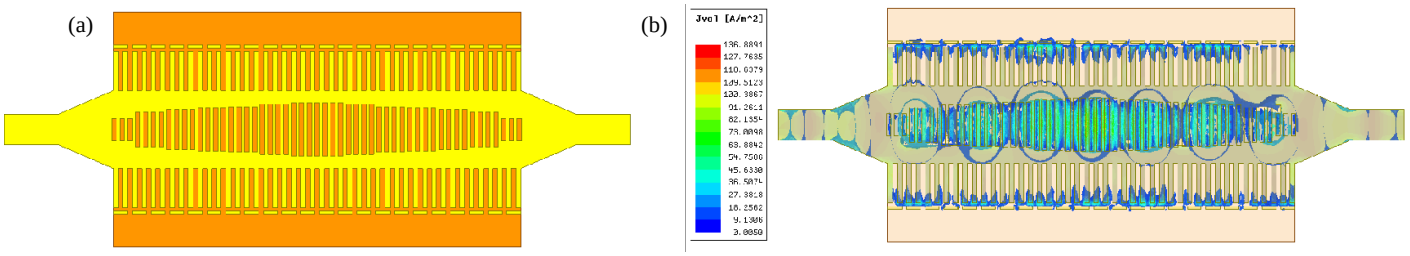

FIGURE 6. The proposed antenna top view with simulated electric field distribution at 24.7 GHz.

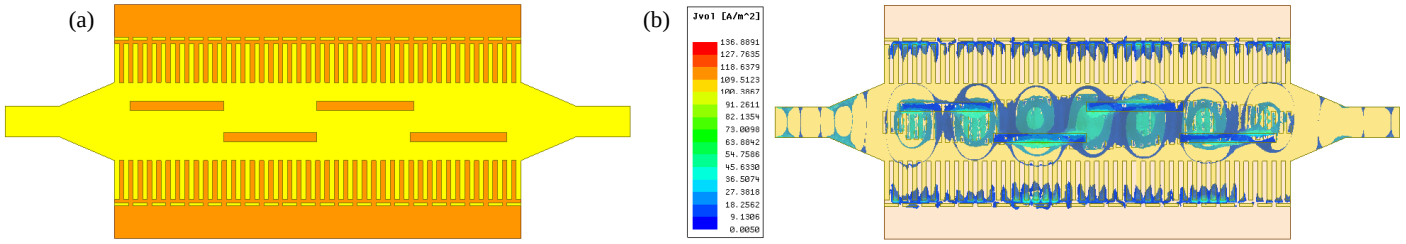

FIGURE 7. The proposed antenna bottom view with simulated electric field distribution at 24.7 GHz.

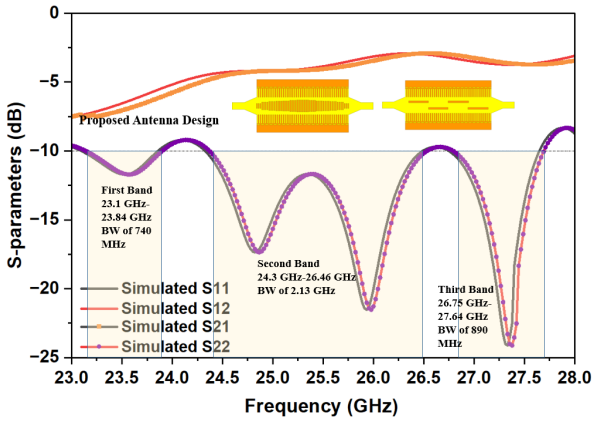

FIGURE 8. Simulated S-parameter response of a proposed antenna with a bandwidth of 740 MHz, 2.13 GHz and 890 MHz (at 23.1 GHz–23.84 GHz), (24.3 GHz–26.46 GHz) and (26.75 GHz–27.64 GHz).

At each band, a simulated wide bandwidth is achieved, i.e., 740 MHz (at 23.1 GHz–23.84 GHz), 2.13 GHz (at 23.1 GHz–23.84 GHz), and 890 MHz, as shown in Fig. 8. Fig. 8 depicts S-parameter results of the proposed antenna. The electric field distribution at 24.7 GHz is shown in Fig. 6 (top view) and Fig. 7 (bottom view). To enable beam steering, longitudinal periodic rectangular slots of length $\lambda/2$ are etched on the bottom ground plane, where λ is the operating wavelength at 24.7 GHz, and the slot width is approximately $\lambda/10$. The guided wave traveling along the electrical walls reflects from the edge of the bottom slot and radiates outward when Port 1 is excited. This results in near broadside radiation at 24.7 GHz, see Fig. 9(a) and Fig. 10(a). At 25.9 GHz and 27.3 GHz band, the wave propagates from port 1 to port 2 such that an end fire radiation pattern is achieved, see Figs. 9(b), (c) and Figs. 10(b), (c). Thus, the proposed antenna radiates in end fire direction at 25.9 GHz and 27.3 GHz and radiates in near broadside direction at 24.7 GHz.

Fig. 10 shows beam steering at three resonant frequency bands, when port 1 is excited (Figs. 10(a), (b), and (c)), when port 2 is excited (Figs. 10(d), (e), and (f)) and when both ports 1 and 2 are excited (Figs. 10(g), (h), and (i)). Thus, by varying the port excitation the beam steering is achieved.

Figure 11 shows measured and simulated S_{11} and S_{21}-parameters of the proposed antenna. The S_{11} and S_{22} are the same, and similarly S_{12} and S_{21} are the same. SMA coaxial 50 ohm connector is soldered at port-1 and port-2. The precise fabrication, calibration, and measurement help to achieve matching frequency bands at 24.7 GHz, 25.9 GHz, and 27.3 GHz, with good impedance matching of -36 dB achieved at 25.8 GHz. A measured wide bandwidth of 3.36 GHz is achieved at the first resonant band, i.e., 23.1 GHz to 26.85 GHz and 700 MHz bandwidth from 27.06 GHz to 27.76 GHz. A slight shift of resonant frequency band is seen at 27.3 GHz but with good return loss of 28.2 dB. The difference between measured and simulated transmission coefficients is shown in Fig. 11, due to phase cable losses, conductor loss, and fabrication errors. The 3D polar plots are shown in Fig. 10, which shows the steering of beams from $+90°$ to $-90°$ by varying the excitation of ports.

When port-1 is excited, the main lobe beam radiates at 157° (near broadside direction, half-power bandwidth (HPBW) of 25.9° at first band), at 90° (end fire direction, HPBW of 58.4° at second band) and at 90° (end fire direction, HPBW of 35° at third band). On exciting port-2, the proposed antenna radiates beam at 202° (near broadside direction, HPBW of 25.9° at first band), at $-90°$ (end fire, HPBW of 58.7° at second band), and at $-90°$ (end fire, HPBW of 35°). When both the ports are excited, the beam radiates at 159° and 200° (near broadside, HPBW of 22.2° at first band), at $+90°$ and $-90°$ (end fire direction, HPBW of 53.4° at second band), and at $+90°$ and $-90°$ (end fire direction, HPBW of 50.7° at third band). The 2D plot

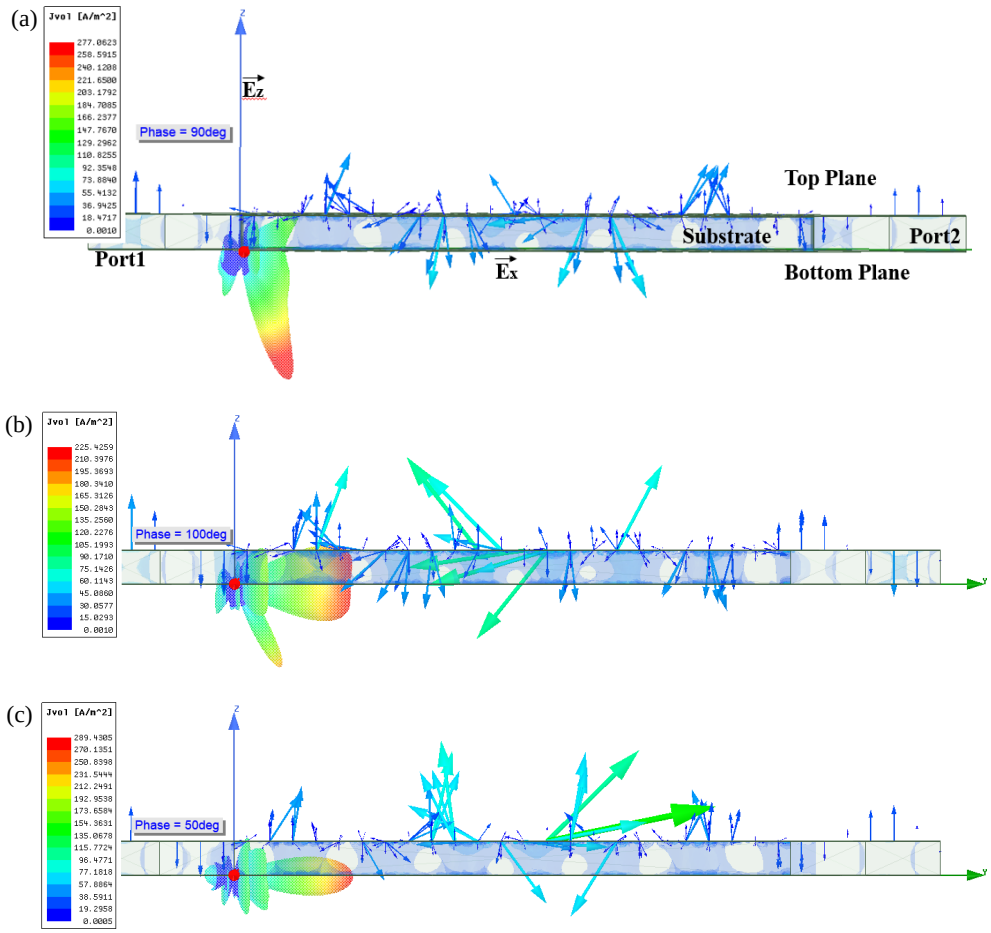

FIGURE 9. Simulated electric field in vector form of proposed antenna at 24.7 GHz, 25.9 GHz and 27.3 GHz.

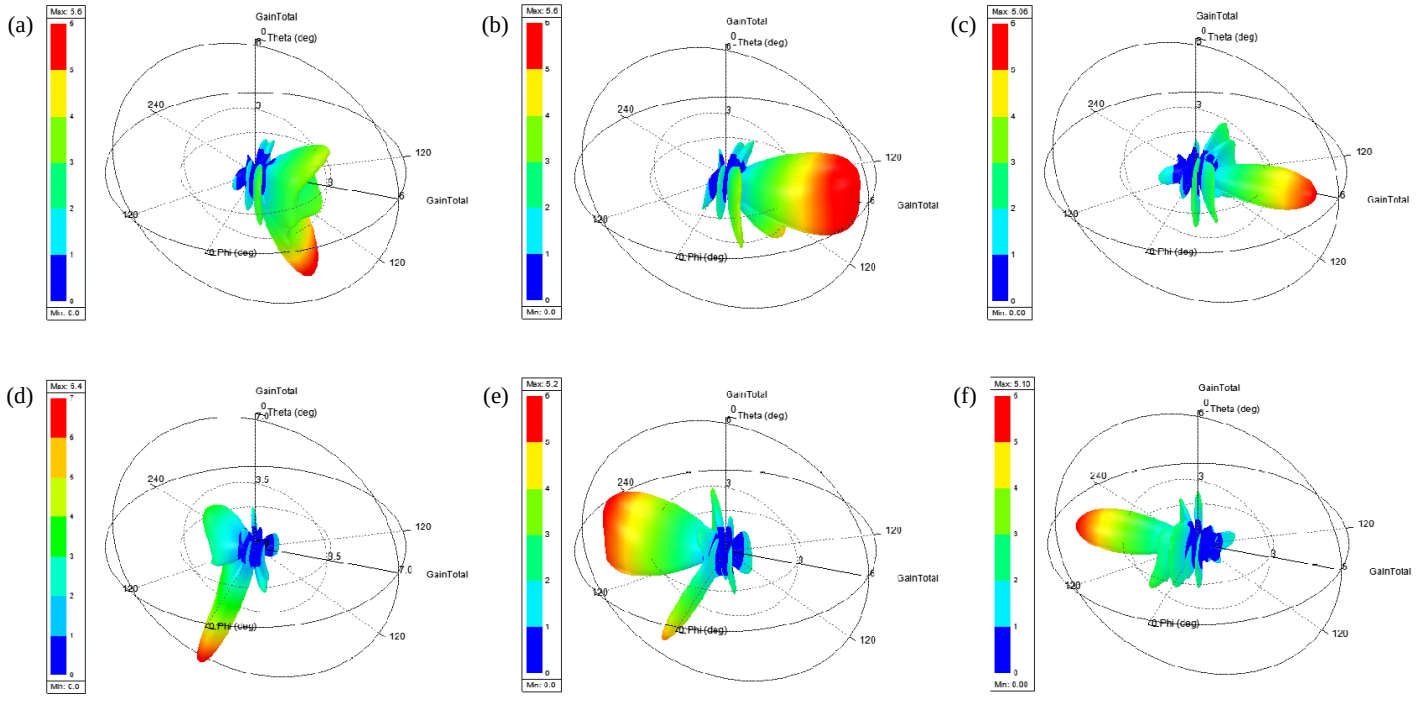

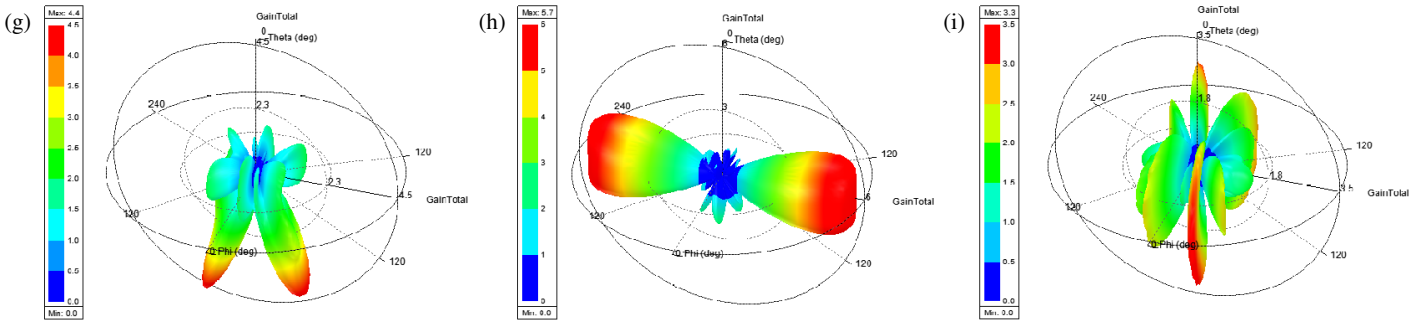

FIGURE 10. The 3D polar plot simulated radiation pattern of the proposed antenna at resonant frequency band when port-1 is excited, i.e., (a) 24.7 GHz, (b) 25.9 GHz, (c) 27.3 GHz, when port-2 is excited, i.e., (d) 24.7 GHz, (e) 25.9 GHz, (f) 27.3 GHz, and when both port-1 & port-2 is excited, i.e., (g) 24.7 GHz, (h) 25.9 GHz, (i) 27.3 GHz.

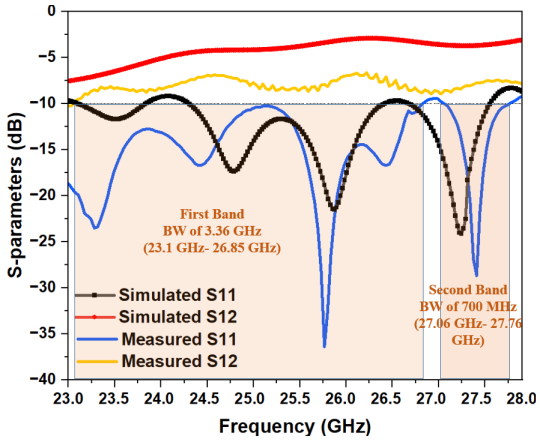

FIGURE 11. Simulated and measured S-parameter results of proposed wideband leaky wave corrugated antenna.

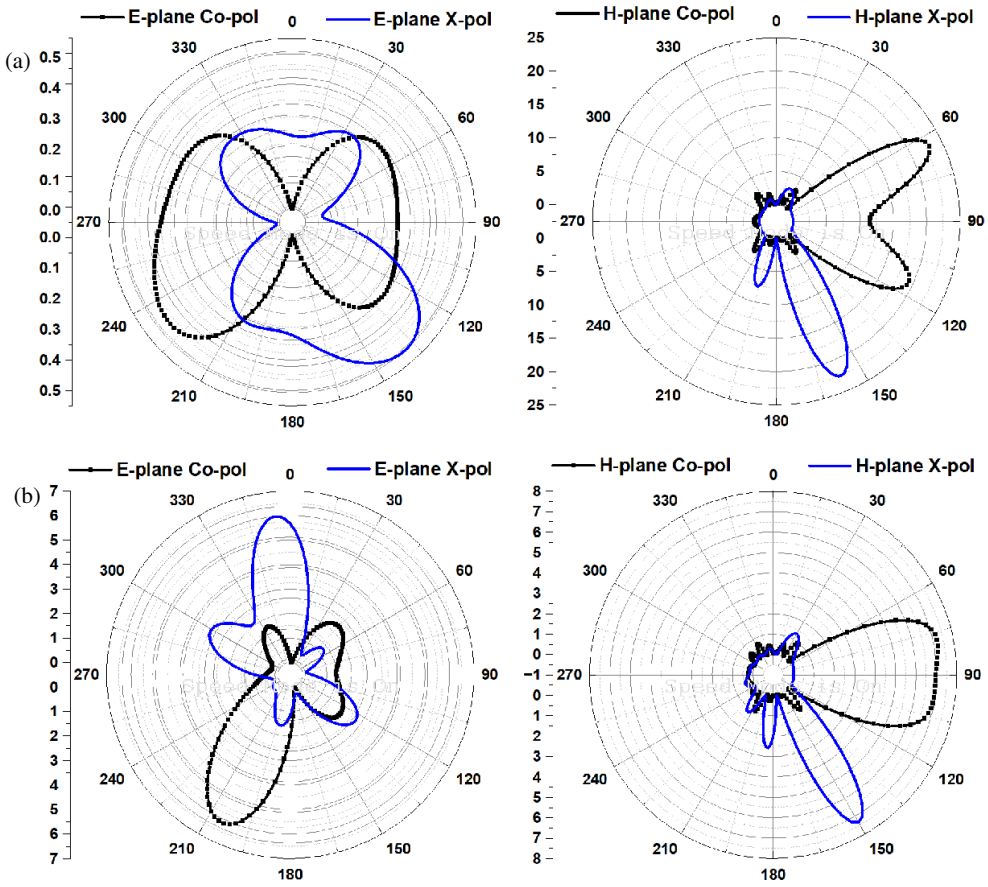

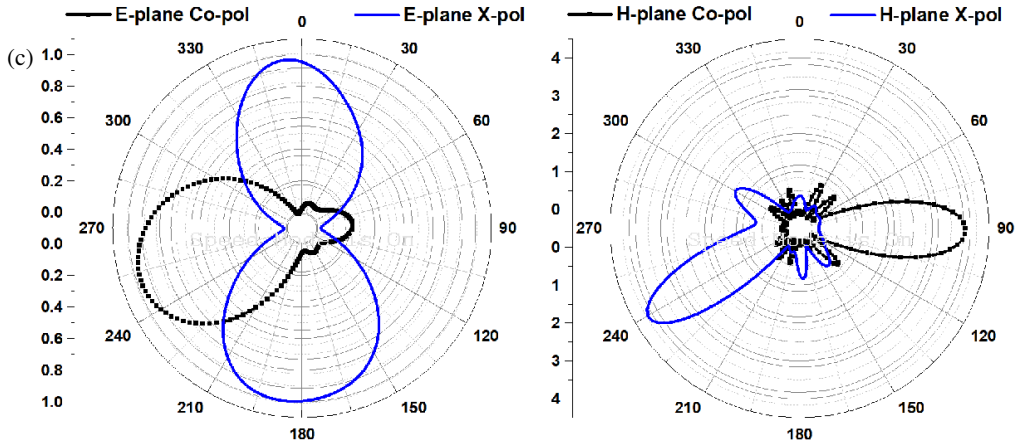

FIGURE 12. Simulated results of 2D plot radiation pattern in E- and H-plane at co-polarization and cross-polarization at (a) 24.7 GHz, (b) 25.8 GHz and (c) 27.3 GHz.

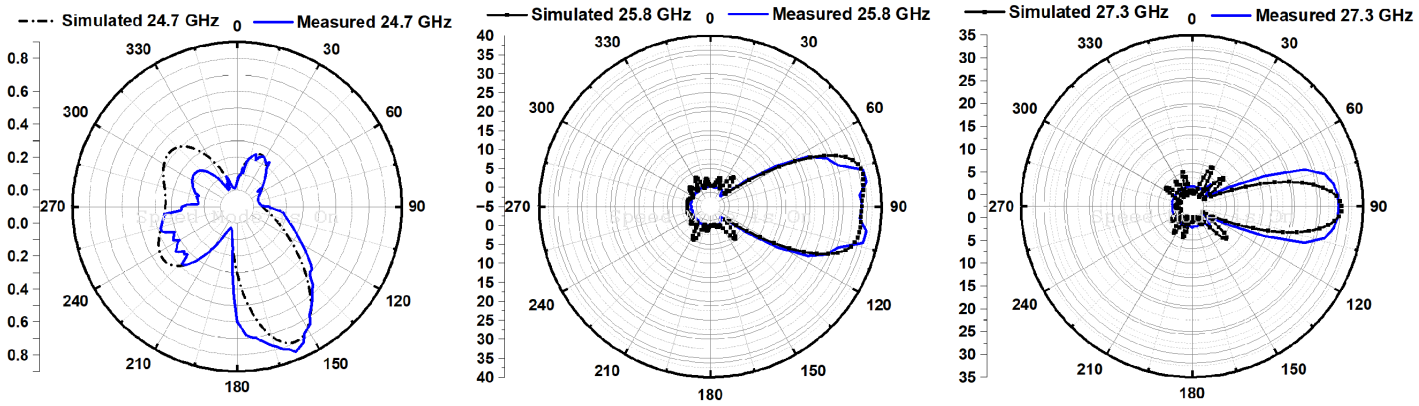

FIGURE 13. Simulated and measured radiation patterns in 2D E-plane at each resonant frequency bands, i.e., 24.7 GHz, 25.8 GHz and 27.3 GHz. (Black color represents simulated and blue color represents measured).

TABLE 2. Comparison of proposed work with existing literature.

Reference	Antenna Size (mm^2 or λ_g)	Resonant Frequency (GHz)	Return loss (dB)	Gain (dBi)
[14]	$2.36\lambda_g \times 22.83\lambda_g \times 0.29\lambda_g$	36	20	12.5
[15]	$0.36\lambda_g \times 6.66\lambda_g \times 0.02\lambda_g$	4.5	11	9.04
[6]	$13.38\lambda_g \times 3.38\lambda_g \times 0.045\lambda_g$	28.5	22	9
This Work	$\mathbf{2.96\lambda_g \times 1.67\lambda_g \times 0.18\lambda_g}$	**24.8** **25.8** **27.3**	**14.38** **18.77** **21.39**	**8** **7.1** **7**

radiation patterns in E and H planes can be seen in Fig. 12(a) 24.7 GHz, (b) 25.8 GHz and (c) 27.3 GHz in co-polarization and cross-polarization planes when antenna 1 is excited.

Figure 13 shows the 2D plot radiation pattern in E-plane measured and simulated results of proposed antenna design at 24.7 GHz, 25.8 GHz, and 27.3 GHz. The near broadside radiation pattern is achieved at 24.7 GHz. A perfect end-fire radiation pattern is achieved at 25.9 GHz and 27.3 GHz in Fig. 13. The proposed leaky wave corrugated antenna prototype is fabricated using PhCNC machine as shown in Figs. 14(a) top view and (b) bottom view. The prototype is connected with SSMA connector and tested using Vector Network Analyzer (VNA) (see Figs. 14(c) and (d)) and anechoic chamber working up to 30 GHz, see Fig. 14(d). A peak realized gain is achieved at 24.7 GHz of 8 dBi, at 25.8 GHz of 7.1 dBi, and at 27.3 GHz of 7 dB when port 1 is excited.

Similarly, a high gain is achieved when port 2 is excited, i.e., 7.9 dBi (at first band), 7 dBi (at second band), and 7 dBi (at third band). But when both the ports are excited, the peak gain is reduced to 6.4 dBi, 7.55 dBi, and 5.2 dBi, due to the distribu-

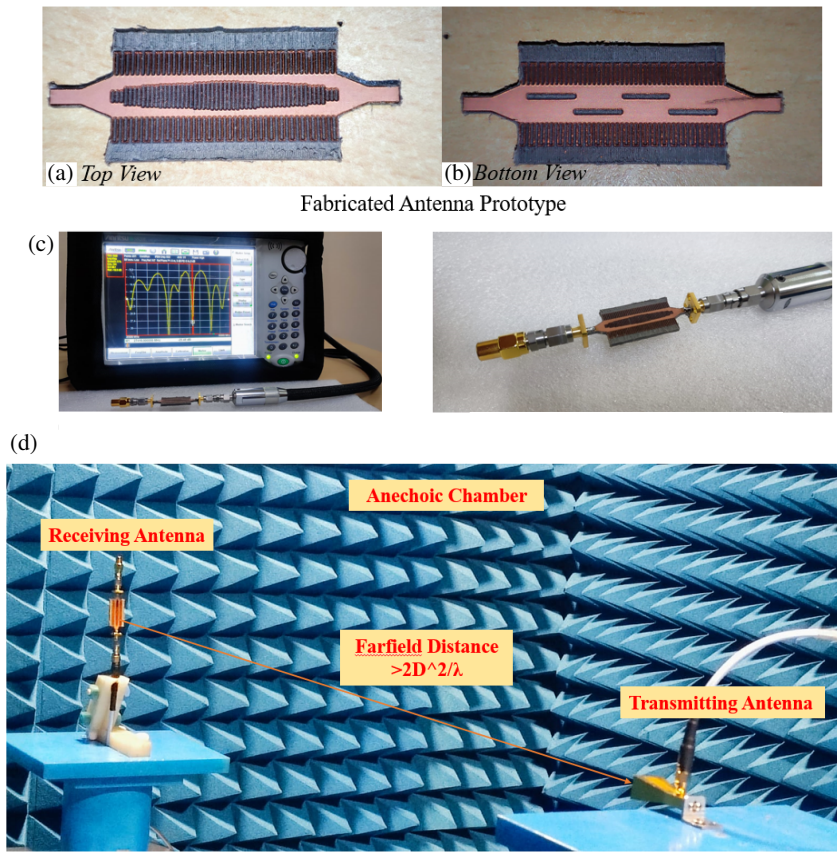

FIGURE 14. Fabricated prototype of proposed antenna with top and bottom view, measurement using vector network analyzer (VNA), antenna connected using SMA coaxial connector and measurement of antenna in anechoic chamber. (a) Top view. (b) Bottom view. (c) VNA test setup; Antenna connected with SSMA. (d) Proposed antenna measurement setup in anechoic chamber.

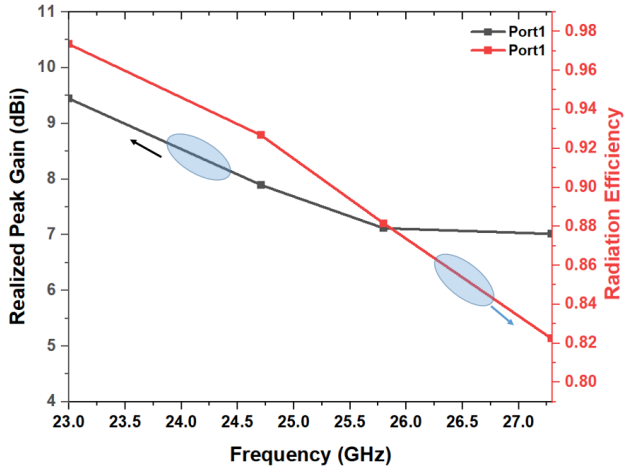

FIGURE 15. Realized peak gain and radiation efficiency of proposed antenna design.

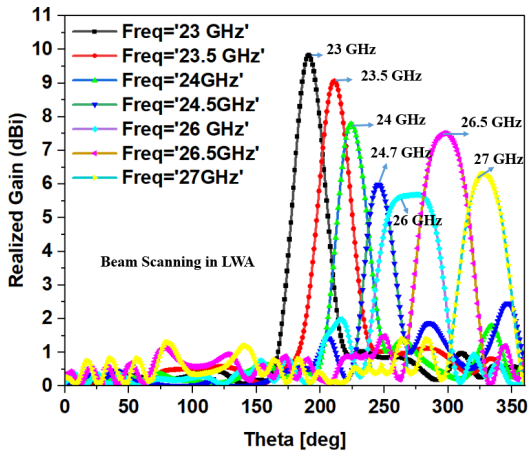

FIGURE 16. Beam steering of proposed antenna at different resonant frequencies with respect to theta and phi = 90 deg, when antenna1 is excited.

tion of power at each resonant band. Fig. 15 and Fig. 16 show realized gains at resonant frequencies, i.e., 23 GHz, 23.5 GHz, 24 GHz, 24.5 GHz, 26.5 GHz, and 27 GHz, with respect to theta and phi = 90°. The beam canning is achieved at 191°, 190°, 198°, 201°, 268°, and 268° at different resonant frequencies. Table 2 shows the comparison of proposed design with existing literature with respect to size, resonant frequency and peak gain. Here, the literature papers compared work on single narrow band with high gain, but proposed design covers a wide bandwidth triple band with high gain at each resonant frequency. The proposed design is a beam steering wide band high gain antenna achieved by bottom longitudinal slots and by varying

the excitation of ports. Voltage standing wave ratio (VSWR) is measured for each band of proposed antenna where the values of VSWR are less than 2 at 23 GHz, 24.7 GHz, 25.8 GHz, and 27.3 GHz. It shows that good matching characteristics are achieved in the proposed antenna design when ports 1 and 2 are excited.

4. CONCLUSION

The proposed beam steering leaky wave periodic stub corrugated antenna design works at resonant frequency bands at 23.1 GHz, 24.7 GHz, 25.9 GHz, and 27.3 GHz with high bandwidths of 3.36 GHz and 700 MHz. The pattern variation observed at 24.7 GHz shows that the antenna radiates close to the broadside direction, while at the other two frequency bands it achieves pure end-fire radiation. The structure employs periodic logarithmic rectangular leaky-wave slots on the top plane and periodic slots on the bottom ground plane. Overall, the proposed configuration forms a compact, periodic stub-corrugated leaky-wave antenna operating in the Ka-band, making it well suited for millimeter-wave applications such as RADAR communication.

REFERENCES

[1] Costantine, J., Y. Tawk, S. E. Barbin, and C. G. Christodoulou, "Reconfigurable antennas: Design and applications," *Proceedings of the IEEE*, Vol. 103, No. 3, 424–437, 2015.

[2] Jackson, D. R., C. Caloz, and T. Itoh, "Leaky-wave antennas," *Proceedings of the IEEE*, Vol. 100, No. 7, 2194–2206, 2012.

[3] Altshuler, E., "The traveling-wave linear antenna," *IRE Transactions on Antennas and Propagation*, Vol. 9, No. 4, 324–329, 1961.

[4] Uchimura, H., T. Takenoshita, and M. Fujii, "Development of a "laminated waveguide"," *IEEE Transactions on Microwave Theory and Techniques*, Vol. 46, No. 12, 2438–2443, 1998.

[5] Deslandes, D. and K. Wu, "Single-substrate integration technique of planar circuits and waveguide filters," *IEEE Transactions on Microwave Theory and Techniques*, Vol. 51, No. 2, 593–596, 2003.

[6] Javanbakht, N., R. E. Amaya, J. Shaker, and B. Syrett, "Reconfigurable SIW-based leaky-wave antenna composed of longitudinal cells," *IEEE Access*, Vol. 9, 102 304–102 311, 2021.

[7] Liu, J., D. R. Jackson, Y. Li, C. Zhang, and Y. Long, "Investigations of SIW leaky-wave antenna for endfire-radiation with narrow beam and sidelobe suppression," *IEEE Transactions on Antennas and Propagation*, Vol. 62, No. 9, 4489–4497, 2014.

[8] Karmokar, D. K., Y. J. Guo, P.-Y. Qin, S.-L. Chen, and T. S. Bird, "Substrate integrated waveguide-based periodic backward-to-forward scanning leaky-wave antenna with low cross-polarization," *IEEE Transactions on Antennas and Propagation*, Vol. 66, No. 8, 3846–3856, 2018.

[9] Kuznetcov, M. V., S. K. Podilchak, M. Poveda-García, P. Hilario, C. A. Alistarh, G. Goussetis, and J. L. Gómez-Tornero, "Compact leaky-wave SIW antenna with broadside radiation and dual-band operation for CubeSats," *IEEE Antennas and Wireless Propagation Letters*, Vol. 20, No. 11, 2125–2129, 2021.

[10] Chen, D. G. and K. W. Eccleston, "Substrate integrated waveguide with corrugated wall," in *2008 Asia-Pacific Microwave Conference*, 1–4, Hong Kong, China, 2008.

[11] Wen, W.-W. and F. Xu, "A reconfigurable leaky-wave antenna based on corrugated SIW with fix-frequency wide range beam-scanning," in *2022 International Conference on Microwave and Millimeter Wave Technology (ICMMT)*, 1–3, Harbin, China, 2022.

[12] Chen, K., Y. H. Zhang, S. Y. He, H. T. Chen, and G. Q. Zhu, "An electronically controlled leaky-wave antenna based on corrugated SIW structure with fixed-frequency beam scanning," *IEEE Antennas and Wireless Propagation Letters*, Vol. 18, No. 3, 551–555, 2019.

[13] Lin, Y., Y. Zhang, H. Liu, Y. Zhang, E. Forsberg, and S. He, "A simple high-gain millimeter-wave leaky-wave slot antenna based on a bent corrugated SIW," *IEEE Access*, Vol. 8, 91 999–92 006, 2020.

[14] Hu, W., D. Jiang, C. Zhang, Z. Zhang, B. Yan, C. Xu, W. Yang, Z. Guo, W. Zhang, G. Wang, and C. Fan, "Reconfigurable holographic leaky-wave antenna based on liquid crystal materials," *Microwave and Optical Technology Letters*, Vol. 66, No. 2, e34044, 2024.

[15] Xi, B., Y. Li, Z. Liang, S. Zheng, Z. Chen, and Y. Long, "Periodic fixed-frequency staggered line leaky wave antenna with wide-range beam scanning capacity," *IEEE Access*, Vol. 7, 146 693–146 701, 2019.

[16] Lou, T., X.-X. Yang, H. Qiu, Q. Luo, and S. Gao, "Low-cost electrical beam-scanning leaky-wave antenna based on bent corrugated substrate integrated waveguide," *IEEE Antennas and Wireless Propagation Letters*, Vol. 18, No. 2, 353–357, 2019.

[17] Deslandes, D., "Design equations for tapered microstrip-to-substrate integrated waveguide transitions," in *2010 IEEE MTT-S International Microwave Symposium*, 704–707, Anaheim, CA, USA, 2010.

[18] Kim, M., J. Shim, B. Bae, and J. Cheon, "Novel via-less substrate integrated waveguide (SIW) structure using EMI shielding film," in *2024 IEEE Asia-Pacific Microwave Conference (APMC)*, 1209–1211, Bali, Indonesia, 2024.

[19] Sirigineedi, A., S. Bhoopalan, M. Raveendra, U. Saravanakumar, and T. S. Babu, "Via's based parametric analysis of SIW antenna for multiband performance," in *2021 Second International Conference on Electronics and Sustainable Communication Systems (ICESC)*, 644–648, Coimbatore, India, 2021.

[20] Tewari, N., N. Joshi, and S. Srivastava, "A novel reconfigurable H-plane horn leaky wave substrate integrated waveguide MIMO antenna for K band," *AEU — International Journal of Electronics and Communications*, Vol. 170, 154832, 2023.

[21] Agrawal, T. and S. Srivastava, "Ku band pattern reconfigurable substrate integrated waveguide leaky wave horn antenna," *AEU — International Journal of Electronics and Communications*, Vol. 87, 70–75, 2018.

[22] Bhowmik, W., S. Srivastava, and L. Prasad, "Design of multiple beam forming antenna system using substrate integrated folded waveguide (SIFW) technology," *Progress In Electromagnetics Research B*, Vol. 60, 15–34, 2014.

[23] Bansal, A., C. J. Panagamuwa, and W. G. Whittow, "Millimeter-wave beam steerable slot array antenna using an inter-digitated capacitor based corrugated SIW," *IEEE Transactions on Antennas and Propagation*, Vol. 70, No. 12, 11 761–11 770, 2022.

[24] Liu, J. and J. Liang, "Gain enhancement of transversely slotted substrate integrated waveguide leaky-wave antennas based on higher modes," *IEEE Transactions on Antennas and Propagation*, Vol. 69, No. 8, 4423–4438, 2021.